Desalination and Water Treatment
www.deswater.com
doi: 10.1080/19443994.2016.1172984

57 (2016) 29264–29273
December

Taylor & Francis
Taylor & Francis Group

Recovery and application of heavy metals from pickling waste liquor (PWL) and electroplating wastewater (EPW) by the combination process of ferrite nanoparticles

Dan Chen*, Qian Li, Li Shao, Fan Zhang, Guangren Qian

School of Environmental and Chemical Engineering, Shanghai University, No. 99, Shangda Road, Shanghai 200444, China, Tel. +86 2166137784, emails: dchen@shu.edu.cn, chendan_shu@hotmail.com (D. Chen), 18717917816@163.com (Q. Li), 13701663658@163.com (L. Shao), 601472100@qq.com (F. Zhang), grqian@shu.edu.cn (G. Qian)

Received 9 December 2015; Accepted 24 March 2016

ABSTRACT

Heavy metal contamination in wastewater poses a severe threat to the environment and public health. Magnetic iron-based materials are effective for heavy metal wastewater treatment, resources conservation, and recycling of metal ions. In the present work, two kinds of heavy metal wastewater were used to fabricate magnetically separable $MnFe_2O_4$ and $CuFe_2O_4$ as catalysts. The obtained catalysts were characterized by scanning electron microscopy, X-ray diffractometry, vibrating sample magnetometer, and X-ray photoelectron spectroscopy. Results showed that $MnFe_2O_4$ and $CuFe_2O_4$ MNPs could effectively activate peroxymonosulfate (PMS) to generate powerful sulfate radicals ($SO_4^{-\cdot}$) for Rhodamine B (RhB) removal. More than 99% of RhB (10 mg/L) was degraded within 20 min using 0.4 g/L $MnFe_2O_4$ MNPs and 0.2 g/L PMS. The most effective pH for RhB degradation by PMS/WB-$MnFe_2O_4$ was 3. And under the condition of catalysts loading (0.40 g/L), dye concentration (10 mg/L), PMS = 0.2 g/L and $T = 25$°C, the stability and reusability of $MnFe_2O_4$ and $CuFe_2O_4$ MNPs was investigated. Recycled WB-$MnFe_2O_4$ MNPs showed strong activity in RhB degradation and its activity remained almost unchanged in eight cycles, while the activity of WB-$CuFe_2O_4$ MNPs dropped down after three cycles.

Keywords: Heavy metal wastewater; Ferrite; Rhodamine B; Peroxymonosulfate activation; Sulfate radical

1. Introduction

Over the last decade, with the rapid development of industries, such as metal plating facilities, fertilizer industries, mining operations, and paper industries [1], heavy metal wastewater discharge into the environment is becoming the special concern as a result of the freshwater crisis. Therefore, the removal of heavy metal ions from wastewater has become a crucial issue. Various traditional technologies have been adopted to remove the heavy metal ions from wastewater [2–6]. Recently, in order to utilize those heavy

*Corresponding author.

Presented at the 8th International Conference on Challenges in Environmental Science & Engineering (CESE-2015) 28 September–2 October 2015, Sydney, Australia

metal ions, electrodialysis (ED), electrolysis (EL), and electrodeionization (EDI), etc. [7–12], which could concentrate the low concentration of heavy metals (0.5–1.5 g/L), a minimum of 30% of the nickel within the spent pickling acid can be recovered, and the remaining part of filter liquor can be diluted for reuse [13], were applied to recover nickel from rinse water. However, during the process of removal, the potential application value of the heavy metal of wastewater is ignored. Another new method that could simultaneously remove iron from cyanide-containing heavy-metal wastewaters (Ni, Zn, Cr, and Fe) and pickle acid liquor (Fe) by fabricating layered double hydroxide was reported in the literature [14,15]. The formation of ferrite was early applied to remove heavy metals from acid mine drainage treatment and industrial wastewaters [16,17]. Recently, Chen et al. [18] also investigated that heavy metal ions can form two kinds of materials, ferrite and heavy metal-layered double hydroxide via two-step microwave hydrothermal method. Because of the relative stable structure of spinel ferrite, the synthetic process with Fe^{3+} and other M^{2+} could remove heavy metal ions from the effluent [19]. At the same time, the synthesized solid phase can apparently reduce the leaching of heavy metals [20]. The magnetic property of spinel ferrite has an advantage for its separation from aqueous solution [21].

Based on the concept of resources reclamation, the magnetic wastewater-based (WB) nanoparticles could be reused in other circumstances (e.g. environmental remediation, high-density magnetic storage, heterogeneous catalysts for organic degradation) [22–24]. In order to comply with environmental regulations, it is important to fabricate the WB materials in a proper way. At present, the organics in wastewaters from chemical and related industries have become a great concern due to degradation of these contaminants being very slow or ineffective and not environmentally compatible with conventional processes [25]. Rhodamine B, a toxic and considerable damage organic pollutant, is severely causing threat to the circumstance and the risk posed to the human health even at low concentrations [26]. So, it is an imperative appeal to degrade these POPs before its discharging into the environment. As one of the most promising methods, sulfate radicals activated from peroxymonosulfate (PMS) become a potential alternative, which are more cost-effective and environmentally friendly. Heterogeneous catalytic oxidizing material energizing peroxymonosulfate (PMS) to produce sulfate radicals for degradation of organic compounds systems have recently attracted much interest due to easily recovery and reuse of the catalysts [27–30]. Kanchi et al. [31,32] reported a modified activated carbon as an eco-friendly adsorbent (second stage waste) for the removal of Cr(III) ions from aqueous solutions.

In this work, two kinds of wastewater laden, pickling waste liquor (PWL) and electroplating wastewater (EPW) were employed to fabricate magnetically nanoscale ferrites $MnFe_2O_4$ and $CuFe_2O_4$. The as-prepared WB-$MnFe_2O_4$ MNPs and WB-$CuFe_2O_4$ MNPs were used as catalysts for activating peroxymonosulfate to generate sulfate radicals. Rhodamine B was chosen as the target compound to evaluate its catalytic activity. Some important affecting factors including initial pH, catalyst, and oxone dosage were selected to investigate the catalytic activity of WB-$MnFe_2O_4$ MNPs and WB-$CuFe_2O_4$ MNPs. In addition, the stability, reusability, and degradation mechanism of the catalysts were also evaluated.

2. Materials and methods

2.1. Materials

Two typical heavy metal wastewater (PWLs and EPWs) were obtained from Shanghai Second Steel Co., Ltd and Shanghai Sheng Xing electroplating factory (Shanghai, China), respectively. The main components of two wastewaters were shown in Table 1. Rhodamine B (>99.9%, Formula: $C_{28}H_{31}ClN_2O_3$, Formula weight: 479.02) and Oxone (Formula: $KHSO_4{\cdot}K_2SO_4{\cdot}KHSO_5$, Formula weight: 614.7) were purchased from Sigma–Aldrich, China. All the other chemicals were analytically graded and were provided from Shanghai Chemical Reagent Company, China, including $MnCl_2{\cdot}4H_2O$, $Na_2B_4O_7{\cdot}10H_2O$, H_3BO_3, NaOH, and ethanol. The water used in all experiments was purified by a Milli-Q system.

2.2. Preparation of $CuFe_2O_4$ and $MnFe_2O_4$ nanoparticles from wastewater

The experimental procedure for the synthesis of wastewater-based $CuFe_2O_4$ and $MnFe_2O_4$ was similar to that described in the literature [33]. In this research, the wastewater-based $CuFe_2O_4$ and $MnFe_2O_4$ have been prepared by following the reported standard protocol by co-precipitation of M^{2+} and M^{3+} in water in the presence of sodium hydroxide. Typically, a mL of PWL and b mL of EPW were mixed together in molar ratio of M^{2+}:M^{3+} = 1:2, which was then dropped slowly into 100 ml 3 M NaOH solution at the temperature of 95℃. After aging for 2 h with continuous stirring, the mixture was filtered, washed, and dried at 60℃ for 12 h.

Table 1
Components of main metals in two typical wastewaters

	The heavy metal ions concentration (mg/L)						
	Fe^{2+}	Fe^{3+}	Cu^{2+}	Mn^{2+}	Cr^{3+}	Zn^{2+}	Ni^{2+}
PWL	41,974.50	2,209.19	UD[a]	219.60	4,183.21	UD	518.53
EPW	UD	UD	174.67	UD	UD	UD	10.39

[a]UD related to undetected.

2.3. Catalytic degradation experiment

In this investigation, the performance of the catalyst refers to the catalytic activity and stability, with the catalytic activity and stability represented by the decolorization efficiency of dye RhB, and the leaching of metal elements in aqueous solution, respectively. The leaching was represented by leaching concentration (dissolved metal elements concentration in solution) and leaching percent (% loss of metal elements in solution), respectively.

2.3.1. Batch reaction

The catalytic degradation of dye experiments were carried out at ambient temperature (~25˚C) in a 500-mL reactor with 200 mL of RhB solution (10.0 mg/L unless otherwise stated) which were placed on a mechanical rabbling plate. Tetra-borate rather than phosphate was used as a buffer in most of the reactions, because phosphate usually is a strong coordinate for transition metals. A known amount of oxone was added to the RhB solution, and then a given amount of the catalyst was added into the reactor to start the reaction with catalyst dosage ranging from 0.04 to 0.4 g/L. The reactor was covered to avoid volatilization. At fixed reaction time intervals, reaction mixture samples (about 5 mL for each) were drawn from the suspension, quenched with excess sodium nitrite to prevent further reaction, and then centrifuged. At the end of reaction, samples were quenched with excess sodium nitrite and filtered with filter paper to analysis.

2.3.2. The recycle of the catalyst

After each run, the spent catalyst was filtered from the reaction mixture with filter paper. Then, all the materials were dried at 100˚C for 12 h and a recyclable catalyst is produced. Several parallel reactions were carried out, at the same time, the recovery amount of catalyst should be enough for the next run. Generally, the experiments were conducted in duplicate and the errors of the experimental results were below 3%.

2.3.3. Analysis

The RhB concentrations in aqueous solution were determined by means of UV–vis spectrophotometry (UV-4802H) at 554 nm and the UV–vis absorption spectra of the selected RhB aqueous solutions were recorded. Morphological images of the samples were taken by the scanning electron microscope (SEM, Hitachi H-800). The metal elements in solution were measured by an inductively coupled plasma (ICP-AES, Shimadzu, ICPS-7510) emission spectrometer (Prodigy). The magnetic properties of synthesized materials were measured by the vibrating sample magnetometer (VSM 7407 type, Lake Shore, America). The total organic carbon (TOC multi N/C 2100, Analytik Jena, Germany) of the selected samples was measured by Shimadzu TOC-5000A analyzer.

2.4. Catalyst characterization

pH_{pzc} (pH at which the surface is zero-charged) was determined with acid−base titration. The field-dependent magnetization (M−H) at room temperature was measured with a superconductor quantum interference magnetometer SQUID-VSM. The morphology of the oxide particles was examined from SEM pictures taken on a Quanta 200 (FEG) scanning electronic microscopy (Fig. 1). XRD on a Rigaku D/max RBX X-ray diffractometer (Model XD-3A, Shimadzu Co., Japan) with Cu K radiation (λ = 0.154 nm, 34 kV, 20 mA) at a scanning rate of 4˚/min in the range of 5–80˚ was used to determine the modification of the crystalline structure of the particles before and after the reaction. Metal oxidation states of wastewater-based $CuFe_2O_4$ and $MnFe_2O_4$ particles before and after reaction were characterized with X-ray photoelectron spectroscopy (XPS) (Kratos AMICUS/ESCA 3400 spectrometer).

3. Results and discussion

3.1. Characterization of wastewater-based $CuFe_2O_4$ and $MnFe_2O_4$ MNPs

The SEM observation (Fig. 1) showed that the wastewater-based $MnFe_2O_4$ MNPs were composed of

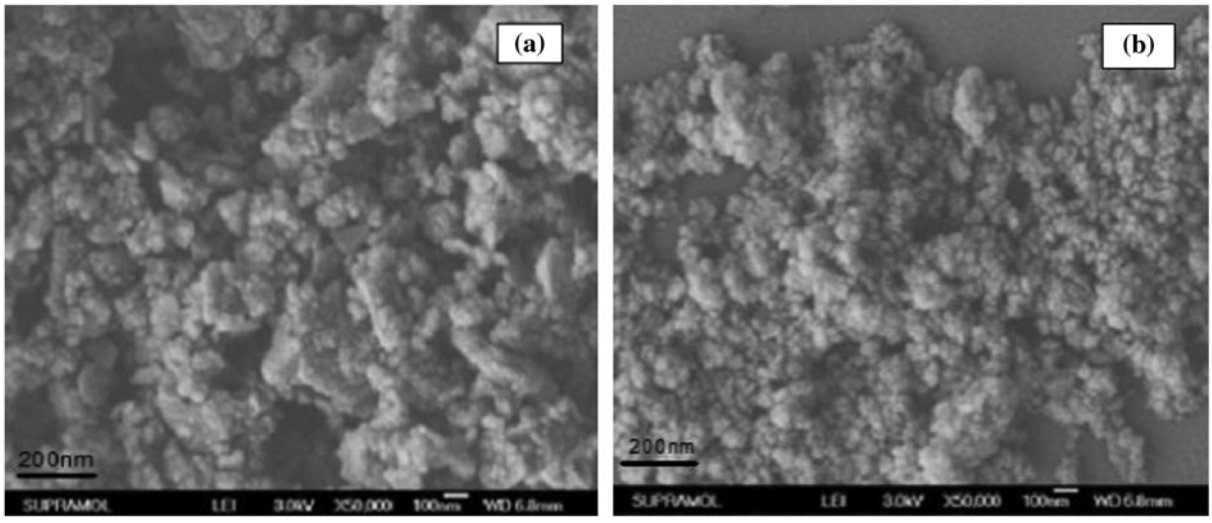

Fig. 1. SEM of (a) wastewater-based $CuFe_2O_4$ MNPs and (b) wastewater-based $MnFe_2O_4$ MNPs.

sphere particles with particle sizes of about 30–50 nm (Fig. 1(b)), being much smaller than the as-prepared $CuFe_2O_4$ MNPs (100–150 nm) (Fig. 1(a)). XRD (Fig. 2) was employed to analyze the crystalline phases of as-prepared samples. It is obvious that wastewater-based $CuFe_2O_4$ and $MnFe_2O_4$ exhibit similar XRD patterns. The diffraction peaks for the wastewater-based $MnFe_2O_4$ MNPs corresponded well with spinel-type $MnFe_2O_4$ (JCPDS 73-1964) [34,35]. The XRD pattern of $CuFe_2O_4$ MNPs presented three intense diffraction peaks at 2θ angle of 34.718, 35.861, and 62.156, being well matched with the published JCPDS data (JCPDS File No. 34-0425) for the tetragonal $CuFe_2O_4$ spinel [36], while no typical diffraction peak of CuO or Fe_2O_3 is observable in both particles, confirming the absolute transformation of the crystalline phase of MNPs and the structures of $CuFe_2O_4$ and $MnFe_2O_4$. The M–H curves (Fig. 3) demonstrated that WB-$MnFe_2O_4$ and WB-$CuFe_2O_4$ were paramagnetic with the saturation moment per unit mass of about 17.85 and 4.10 emu/g, respectively. Both of the particle sizes and M–H curves were bigger compared to previous reports [37]. When the external magnetic field is added, ferrite particles can be found exhibiting a markedly magnetic response.

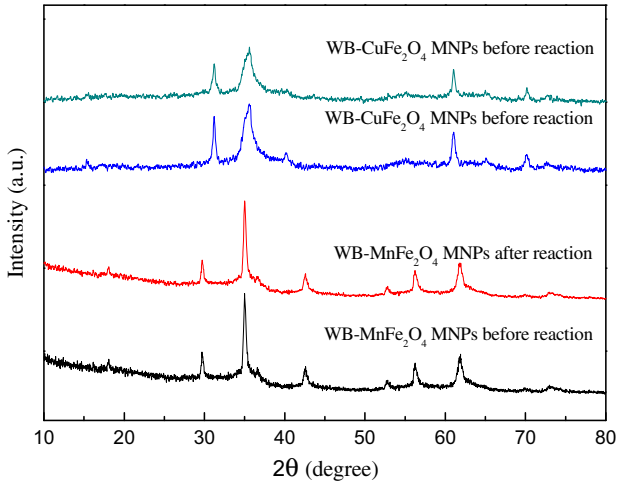

Fig. 2. XRD of wastewater-based $CuFe_2O_4$ and $MnFe_2O_4$ MNPs before and after degradation.

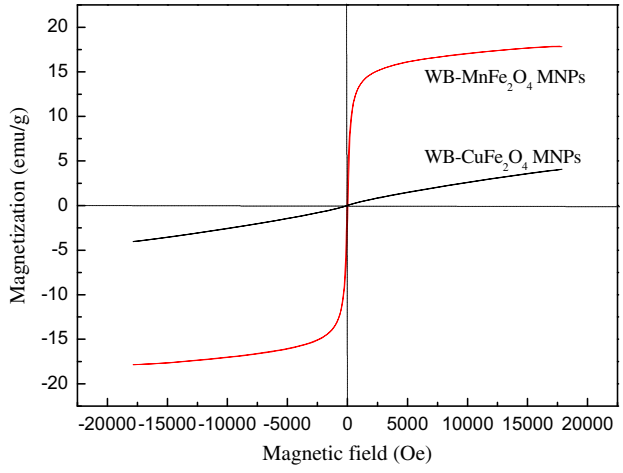

Fig. 3. VSM of wastewater-based $CuFe_2O_4$ and wastewater-based $MnFe_2O_4$ MNPs.

3.2. Catalytic activity comparison of wastewater-based $CuFe_2O_4$ and $MnFe_2O_4$ MNPs

Fig. 4 gets an insight on the kinetic data of organic pollutants degradation with high value of regressions coefficient in different systems. Nearly no prominent change of RhB concentration was noticed and the degradation rate in the PMS system alone was extremely slow. Less than 24% of RhB was degraded in the absence of any catalyst in 30 min. It is observed that the decolorization of the $MnFe_2O_4$/PMS is faster when compared to $CuFe_2O_4$/PMS. The reaction carried out with the simultaneous use of WB-$MnFe_2O_4$ MNPs and PMS promoted the RhB degradation significantly, yielding a 99% removal of RhB in 20 min, while $CuFe_2O_4$ with a RhB showed removal of 99% in 30 min, which indicated that the catalytic activity of WB-$MnFe_2O_4$ MNPs was better than WB-$CuFe_2O_4$ MNPs. It was interesting that the faster decrease in organic pollutant concentration for the $MnFe_2O_4$/PMS couple reversed the previous investigations, meaning the materials obtained from wastewater may exist other accessible active sites in the process of reaction.

Degradation of RhB fits first-order kinetic model as listed below (Eq. (1)), which was successfully employed to describe the relationship between the degradation rate and the initial concentration of organic pollutant [38]:

$$\ln(C/C_0) = kt \tag{1}$$

In the equation, C and C_0 are the RhB concentrations at time (t) and $t = 0$, respectively, and k is the reaction rate constant. The reaction rate constants of RhB degradation in WB-$MnFe_2O_4$/Oxone/RhB system and WB-$CuFe_2O_4$/Oxone/RhB system were 0.12 and 0.04 min^{-1} when pH was 3, respectively, suggesting that Mn(II) in the structure of WB-$MnFe_2O_4$ plays a more significant role for the activation of PMS in the heterogeneous catalytic system than Cu(II). Additionally, the catalyst could be collected from the solution after the reaction due to the magnetic properties of ferrites.

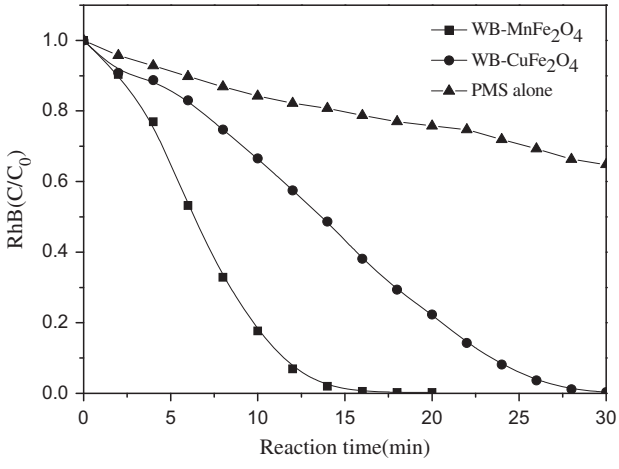

Fig. 4. Catalytic activity of wastewater-based $CuFe_2O_4$ and $MnFe_2O_4$ MNPs (reaction conditions: [RhB] = 10 mg/L, [PMS] = 0.20 g/L, [catalyst] = 0.40 g/L, T = 25°C).

The degradation rate of RhB was remarkably influenced by the reaction pH. Kinetic curves (Fig. 5(c) and (d)), an important operating parameter of dye removal at different pH in the presence of $MnFe_2O_4$/PMS or $CuFe_2O_4$/PMS system, showed that the organics deterioration was inconsistent with the first-order kinetics. RhB degradation was checked in the pH range 3–9. It was obvious that the rate constants (k) of $MnFe_2O_4$ was higher than those of $CuFe_2O_4$ when pH was 3 (Table 2), the decrease of the rate constants mainly could be attributed to the small fraction of SO_5^{2-} existed in the system [34].

3.3. Degradation of Rhodamine B under different pH

In order to reasonably investigate the effect of pH on degradation, we studied the pH conditions of experiment ranging from 3 to 9. When the initial pH was governed to 5, as revealed in Fig. 5, it leaded to generation of the most effective RhB degradation of PMS/WB-$CuFe_2O_4$. This was because of the fact that at acid pH ($pH < pH_{pzc}$), the surface was positively charged, which improved the formation of sulfate radicals [39]. While in the case of PMS/WB-$MnFe_2O_4$ coupled to pH 3, it may be assumed to the formation of active sulfate radicals that were also favored at lower pH in the complicated wastewater-based material system. At alkaline solution, the degradations were hindered significantly by inhibiting the electrostatic force of attraction between the negative charged surface and the PMS species [39], mainly resulting in the decreasing proportion of SO_5^{2-} and the amount of negative surface charge when the pH was above its pH_{pzc} [40,41].

3.4. Stability and reusability of the prepared catalysts

In order to achieve the purpose of practical implementation, it was crucial to evaluate reusability of the catalysts. Under the condition of catalysts loading (0.40 g/L), dye concentration (10 mg/L), PMS = 0.2 g/L and T = 25°C, the particles were reused to perform with successive tests of RhB degradation in the PMS oxidation system (Fig. 6). Recycled WB-$MnFe_2O_4$ MNPs

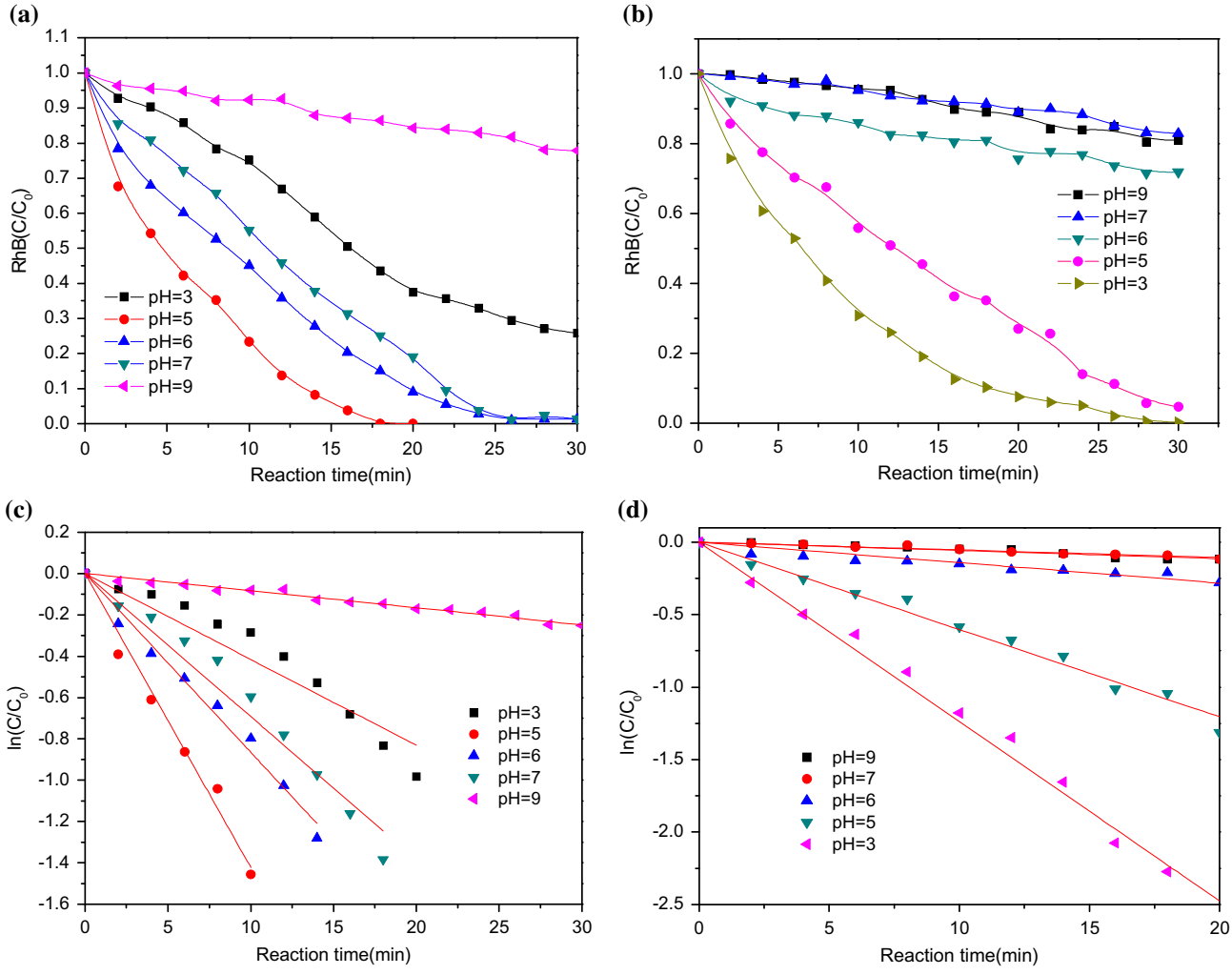

Fig. 5. Degradation of RhB under different pH: (a) and (c) WB-$CuFe_2O_4$ and (b) and (d) WB-$MnFe_2O_4$ (reaction conditions: [RhB] = 10 mg/L, [PMS] = 0.20 g/L, [catalyst] = 0.40 g/L, T = 25°C).

Table 2
The apparent first-order rate constants at various pH levels

	RhB degradation, k (min^{-1})		
	PMS	PMS with WB-$CuFe_2O_4$	PMS with WB-$MnFe_2O_4$
pH 3	0.002 ± 0.0001	0.0416 ± 0.0020	0.1238 ± 0.002
pH 5	0.002 ± 0.0001	0.1422 ± 0.004	0.0603 ± 0.001
pH 6	0.001 ± 0.0001	0.0865 ± 0.002	0.0141 ± 0.0007
pH 7	0.001 ± 0.0001	0.0692 ± 0.002	0.0053 ± 0.0002
pH 9	0.001 ± 0.0001	0.0083 ± 0.0001	0.0057 ± 0.0002

Note: The reaction time was 30 min, and a standard deviation was used as an error of rate constant.

showed strong activity in RhB degradation and its activity remained almost unchanged in eight cycles, while the activity of WB-$CuFe_2O_4$ MNPs dropped down after three cycles due to the rapid absence Cu^{2+} in this heterogeneous catalytic reaction, which was supported by its quick copper leaching in the third cycle reactions, resulting in the decreasing of its degree of crystallinity. The data indicated that Mn(II) sites attached on the

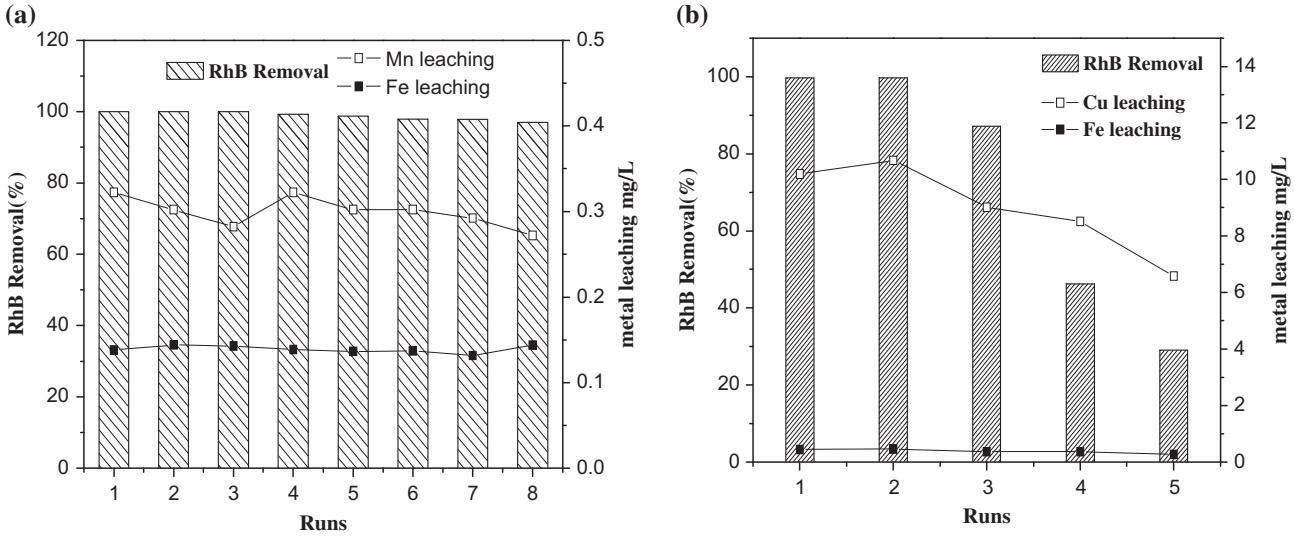

Fig. 6. Catalytic reusability and stability: (a) WB-$MnFe_2O_4$ and (b) $CuFe_2O_4$ MNPs (reaction conditions: [RhB] = 10 mg/L, [PMS] = 0.20 g/L, [catalyst] = 0.40 g/L, T = 25°C).

surface of $MnFe_2O_4$ were more active and stable than those of $CuFe_2O_4$. The lower leaching of Fe(III) of both catalysts manifested that Fe(III) doesn't participate in the process of catalysis. After a series of reactions, there was no apparent change of crystallinity of the $MnFe_2O_4$, which was qualitatively characterized by XRD (Fig. 3). By the way, magnetic separation showed no obvious dissolution of WB-$MnFe_2O_4$ MNPs and WB-$CuFe_2O_4$ MNPs. It can be concluded that the RhB degradation in PMS/$MnFe_2O_4$ are much more applicable for water treatment than PMS/$CuFe_2O_4$.

3.5. Reaction mechanism

For the purpose of understanding the dominant role of radical specie SO_4^{-}·, quenching agents were added into the reaction solution. Two types of reactive radicals, sulfate and hydroxyl radicals [36] generated in the PMS/$MnFe_2O_4$ system were responsible for the degradation of organic pollutants. According to the previous investigations [42], TBA and EtOH were used as quenching agents to identify the major effective radicals in our experiment because of the high and comparable rates of ·OH or SO_4^{-}·.

As shown in Fig. 7, TBA was used as scavenger for ·OH and EtOH was used as scavenger for ·OH and SO_4^{-}·. More than 99% of RhB was degraded in 30 min without the addition of quenching agents. As a comparison, when 0.5 mol/L TBA and 0.5 mol/L EtOH were added, 80 and 72% RhB were removed in 30 min, respectively. The much higher inhibition rate of the RhB degradation by EtOH than by TBA

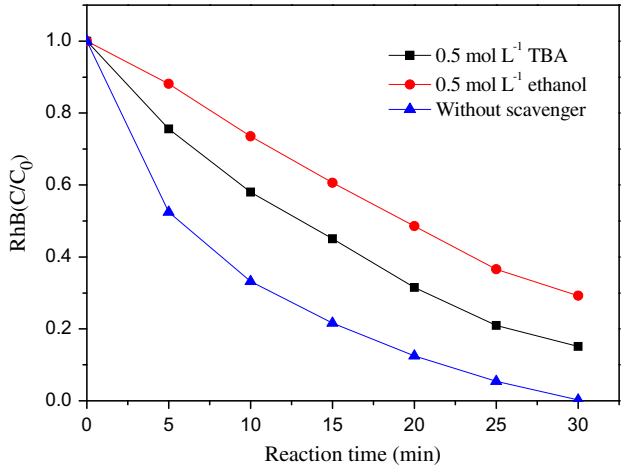

Fig. 7. The degradation kinetics of RhB with different quenching agents (reaction conditions: [RhB] = 10 mg/L, [PMS] = 0.20 g/L, [catalyst] = 0.40 g/L, T = 25°C).

suggests that sulfate radicals played the dominant role during the activation of PMS by $MnFe_2O_4$.

It is believed that the oxidation may induce microphase separation and deactivation of the catalysts and the change of the surface chemical properties after the reaction. The surface characteristics of WB-$MnFe_2O_4$ MNPs before and after catalytic reaction were measured by XPS is necessary.

The reduction of $M^{(n+1)+}$ to M^{n+} by PMS was thermodynamically feasible during the catalytic PMS oxidation with free metal ions (M^{n+}) [43]. Fig. 8 showed the full-scale XPS spectrum (C 1s, O 1s, Mn 2p, and Fe

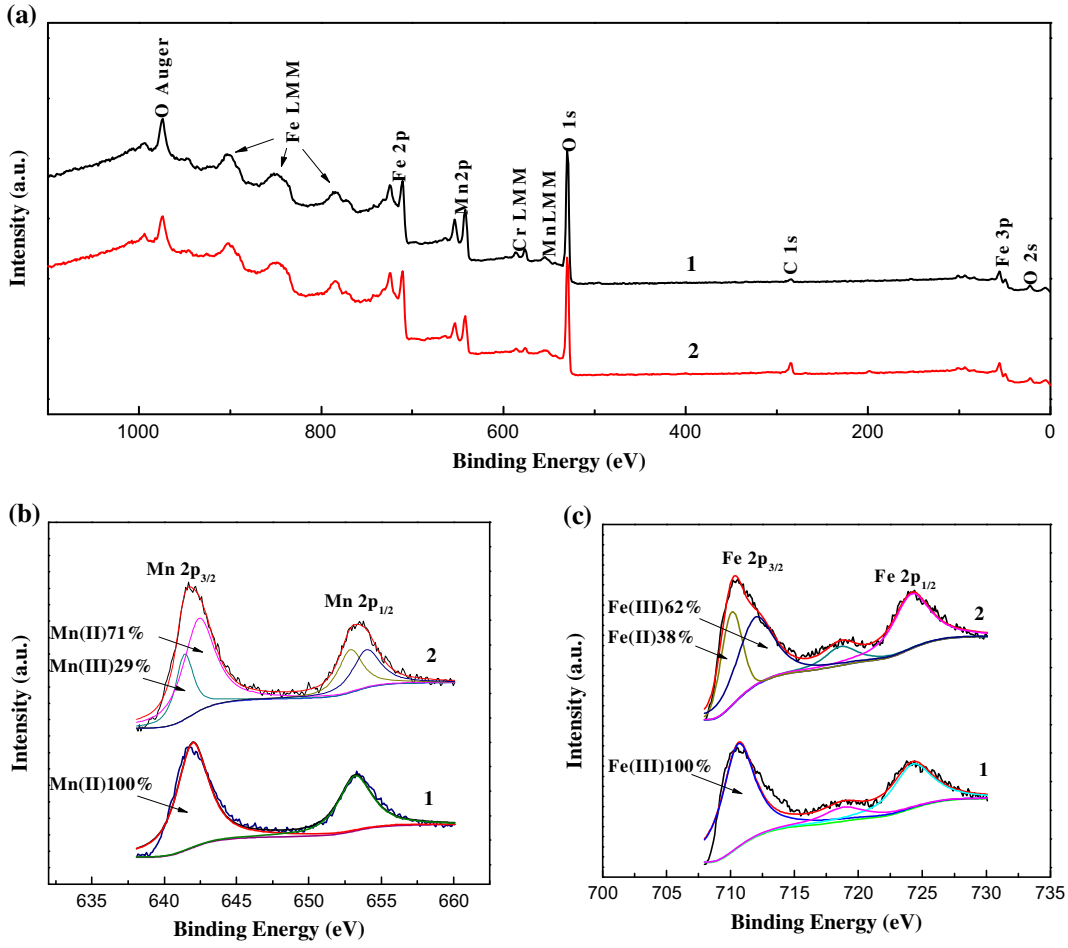

Fig. 8. (a) Wide survey XPS spectra, (b) Mn 2p, and (c) Fe 2p XPS peak envelop of (1) the fresh and (2) used wastewater-based $MnFe_2O_4$ MNPs.

2p) of the WB-$MnFe_2O_4$ MNPs. It was found that the peaks at 642.2 and 653.2 eV are assigned to Mn 2p3/2 and Mn 2p1/2 in the high-resolution XPS spectra of Mn 2p (Fig. 8(b)), respectively. All Fe 2p spectra (Fig. 8(c)) show two main peaks at binding energies of 711.5 (Fe 2p3/2) and 725.1 eV (Fe 2p1/2), which suggested that Mn and Fe species are present in a mixed valence. From the deconvolution of Mn (2p) and Fe (2p) envelops, Mn(III) and Fe(II) were found to account for 29 and 38% of Mn and Fe species, respectively. This suggests that Mn(II) and Fe(III) on surface of the used catalyst were partially transformed to Mn (III) and Fe(II), respectively [30,44]. Thus, it is proven that ≡Mn(II)/≡Mn(III) and ≡Fe(II)/≡Fe(III) are redox couples reacted with PMS to generate $SO_4^{-\cdot}$ in WB-$MnFe_2O_4$ MNPs resulting in high catalytic activity. So, according to the previous work, the activation mechanism of PMS was assumed as follows [45–48]:

$$\equiv Mn(II)\text{–}{}^{-}OH + HSO_5^- \rightarrow \equiv Mn(III)\text{–}{}^{-}OH + SO_4^{-\cdot} \quad (2)$$

$$\equiv Mn(III)\text{–}{}^{-}OH + HSO_5^- \rightarrow \equiv Mn(II)\text{–}{}^{-}OH + SO_5^{-\cdot} + H^+ \quad (3)$$

$$\equiv Fe(II)\text{–}{}^{-}OH + HSO_5^- \rightarrow \equiv Fe(III)\text{–}{}^{-}OH + SO_4^{-\cdot} + OH^- \quad (4)$$

$$\equiv Fe(III)\text{–}{}^{-}OH + HSO_5^- \rightarrow \equiv Fe(II)\text{–}{}^{-}OH + SO_5^{-\cdot} + H^+ \quad (5)$$

4. Conclusion

In this study, $MnFe_2O_4$ MNPs and $CuFe_2O_4$ MNPs have been synthesized from two types of industrial wastewater. These catalysts showed potential capability for catalytic degradation of organic contaminants by PMS as an oxidant. The catalytic performance

showed that $MnFe_2O_4$ MNPs presented higher catalytic activity in RhB degradation than $CuFe_2O_4$ MNPs. The as-prepared $MnFe_2O_4$ MNPs compared with $CuFe_2O_4$ MNPs also demonstrated highly stable performance. Results showed that $MnFe_2O_4$ and $CuFe_2O_4$ MNPs could effectively activate peroxymonosulfate (PMS) to generate powerful sulfate radicals ($SO_4^{-\bullet}$) for Rhodamine B (RhB) removal. More than 99% of RhB (10 mg/L) was degraded within 20 min using 0.4 g/L $MnFe_2O_4$ MNPs and 0.2 g/L PMS. The most effective pH for RhB degradation by PMS/WB-$MnFe_2O_4$ was 3. And under the condition of catalysts loading (0.40 g/L), dye concentration (10 mg/L), PMS = 0.2 g/L and T = 25°C, the stability and reusability of $MnFe_2O_4$ and $CuFe_2O_4$ MNPs was investigated. Recycled WB-$MnFe_2O_4$ MNPs showed strong activity in RhB degradation and its activity remained almost unchanged in eight cycles, while the activity of WB-$CuFe_2O_4$ MNPs dropped down after three cycles. Therefore, WB-$MnFe_2O_4$ MNPs is applicable for the treatment of wastewater containing Rhodamine B and environmental applications.

Acknowledgments

This study was supported by Program for Innovative Research Team in University (No. IRT13078), as well as been supported by National Nature Science Foundation of China Nos. 50704023, 50974086 and 51274138. This study was also funded by China Scholarship Council.

References

[1] F.L. Fu, Q. Wang, Removal of heavy metal ions from wastewaters: A review, J. Environ. Manage. 92 (2011) 407–418.
[2] B. Mokhtari, K. Pourabdollah, Inclusion desalination of alkali metal cations by emulsion liquid membranes and nano-baskets of p-tert-calix[4]arene bearing di-[N-(X)sulfonyl carboxamide] and di-(1-propoxy) in para-cone conformation, Desalination 292 (2012) 1–8.
[3] B. Mokhtari, K. Pourabdollah, Inclusion extraction of alkali metals by emulsion liquid membranes bearing nano-baskets, J. Incl. Phenom. Macrocycl. Chem. 76 (2013) 403–413.
[4] T. Benvenuti, R.S. Krapf, M.A.S. Rodrigues, A.M. Bernardes, J. Zoppas-Ferreira, Recovery of nickel and water from nickel electroplating wastewater by electrodialysis, Sep. Purif. Technol. 129 (2014) 106–112.
[5] T.A. Kurniawan, G.Y.S. Chan, W.H. Lo, S. Babel, Physico-chemical treatment techniques for wastewater laden with heavy metals, Chem. Eng. J. 118 (2006) 83–98.
[6] M.A. Barakat, New trends in removing heavy metals from industrial wastewater, Arabian J. Chem. 4 (2011) 361–377.
[7] A. Mahmoud, A.F.A. Hoadley, An evaluation of a hybrid ion exchange electrodialysis process in the recovery of heavy metals from simulated dilute industrial wastewater, Water Res. 46 (2012) 3364–3376.
[8] K.N. Njau, M. Woude, G.J. Visser, L.J.J. Janssen, Electrochemical removal of nickel ions from industrial wastewater, Chem. Eng. J. 79 (2000) 187–195.
[9] T.A. Green, S. Roy, K. Scott, Recovery of metal ions from spent solutions used to electrodeposit magnetic materials, Sep. Purif. Technol. 22–23 (2001) 583–590.
[10] N. Tzanetakis, W.M. Taama, K. Scott, R.J.J. Jachuck, R.S. Slade, J. Varcoe, Comparative performance of ion exchange membranes for electrodialysis of nickel and cobalt, Sep. Purif. Technol. 30 (2003) 113–127.
[11] M.A.S. Rodrigues, F.D.R. Amado, J.L.N. Xavier, K.F. Streit, A.M. Bernardes, J.Z. Ferreira, Application of photoelectrochemical-electrodialysis treatment for the recovery and reuse of water from tannery effluents, J. Cleaner Prod. 16 (2008) 605–611.
[12] C.S. Peng, Y.Y. Liu, J.J. Bi, H.Z. Xu, A.S. Ahmed, Recovery of copper and water from copper-electroplating wastewater by the combination process of electrolysis and electrodialysis, J. Hazard. Mater. 189 (2011) 814–820.
[13] F. Rögener, M. Sartor, A. Bán, D. Buchloh, T. Reichardt, Metal recovery from spent stainless steel pickling solutions, Resour. Conserv. Recycl. 60 (2012) 72–77.
[14] J.Z. Zhou, Y.Y. Wu, C. Liu, A. Orpe, Q.A. Liu, Z.P. Xu, G.R. Qian, S.Z. Qiao, Effective self-purification of polynary metal electroplating wastewaters through formation of layered double hydroxides, Environ. Sci. Technol. 44 (2010) 8884–8890.
[15] Y.F. Xu, J. Zhang, J.Z. Zhou, C. Chen, Q. Liu, G.R. Qian, Z.P. Xu, CN and heavy metal removal through formation of layered double hydroxides from mixed CN-containing electroplating wastewaters and pickle acid liquor, Chem. Eng. J. 215–216 (2013) 411–417.
[16] W. McKinnon, J.W. Choung, Z. Xu, J.A. Finch, Magnetic seed in ambient temperature ferrite process applied to acid mine drainage treatment, Environ. Sci. Technol. 34 (2000) 2576–2581.
[17] B.E. Morgan, O. Lahav, R.E. Loewenthal, Advances in seeded ambient temperature ferrite formation for treatment of acid mine drainage, Environ. Sci. Technol. 39 (2005) 7678–7683.
[18] D. Chen, Y. Li, J. Zhang, W.H. Li, J.Z. Zhou, L. Shao, G.R. Qian, Efficient removal of dyes by a novel magnetic Fe_3O_4/ZnCr-layered double hydroxide adsorbent from heavy metal wastewater, J. Hazard. Mater. 243 (2012) 152–160.
[19] W.X. Wang, Z.H. Xu, J. Finch, Fundamental study of an ambient temperature ferrite process in the treatment of acid mine drainage, Environ. Sci. Technol. 30 (1996) 2604–2608.
[20] K. Shih, T. White, J.O. Leckie, Nickel stabilization efficiency of aluminate and ferrite spinels and their leaching behavior, Environ. Sci. Technol. 40 (2006) 5520–5526.
[21] P. Xiong, Q. Chen, M.Y. He, X.Q. Sun, X. Wang, Cobalt ferrite-polyaniline heteroarchitecture: A magnetically recyclable photocatalyst with highly enhanced performances, J. Mater. Chem. 22 (2012) 17485–17493.

[22] P.R. Shukla, S.B. Wang, H.Q. Sun, H.M. Ang, M. Tadé, Activated carbon supported cobalt catalysts for advanced oxidation of organic contaminants in aqueous solution, Appl. Catal. B: Environ. 100 (2010) 529–534.
[23] S. Bai, X.P. Shen, X. Zhong, Y. Liu, G.X. Zhu, X. Xu, K.M. Chen, One-pot solvothermal preparation of magnetic reduced graphene oxide-ferrite hybrids for organic dye removal, Carbon 50 (2012) 2337–2346.
[24] Y.J. Yao, Y.M. Cai, F. Lu, F.Y. Wei, X.Y. Wang, S.B. Wang, Magnetic recoverable $MnFe_2O_4$ and $MnFe_2O_4$-graphene hybrid as heterogeneous catalysts of peroxymonosulfate activation for efficient degradation of aqueous organic pollutants, J. Hazard. Mater. 270 (2014) 61–70.
[25] S. Heng, K.L. Yeung, A. Julbe, A. Ayral, J.C. Schrotter, Preparation of composite zeolite membrane separator/contactor for ozone water treatment, Microporous Mesoporous Mater. 115 (2008) 137–146.
[26] S. Christoskova, M. Stoyanova, M. Georgieva, Low-temperature iron-modified cobalt oxide system Part 2. Catalytic oxidation of phenol in aqueous phase, Appl. Catal. A-Gen. 208 (2001) 243–249.
[27] T. Zhang, H.B. Zhu, J.P. Croué, Production of sulfate radical from peroxymonosulfate induced by a magnetically separable $CuFe_2O_4$ spinel in water: Efficiency, stability, and mechanism, Environ. Sci. Technol. 47 (2013) 2784–2791.
[28] Y.J. Yao, Z.H. Yang, D.W. Zhang, W.C. Peng, H.Q. Sun, S.B. Wang, Magnetic $CoFe_2O_4$–Graphene hybrids: Facile synthesis, characterization, and catalytic properties, Ind. Eng. Chem. Res. 51 (2012) 6044–6051.
[29] J. Deng, Y.S. Shao, N.Y. Gao, C.Q. Tan, S.Q. Zhou, X.H. Hu, $CoFe_2O_4$ magnetic nanoparticles as a highly active heterogeneous catalyst of oxone for the degradation of diclofenac in water, J. Hazard. Mater. 262 (2013) 836–844.
[30] Y.B. Ding, L.H. Zhu, N. Wang, H.Q. Tang, Sulfate radicals induced degradation of tetrabromobisphenol A with nanoscaled magnetic $CuFe_2O_4$ as a heterogeneous catalyst of peroxymonosulfate, Appl. Catal. B: Environ. 129 (2013) 153–162.
[31] S. Kanchi, P. Anuradha, B.N. Kumar, K. Gopalakrishnan, P. Ravi, Quantification of Se(IV) and Co(II) in *Macrobrachium lamarrei*, fresh water prawns and their feeding materials, Arabian J. Chem. (2012), doi: 10.1016/j.arabjc.2012.08.001.
[32] S. Kanchi, K. Bisetty, G. Kumar, C.-Y. Lin, T.-S. Chin, Development of green energy waste activated carbon for removal of trivalent chromium: Equilibrium and kinetic modeling, Sep. Sci. Technol. 49 (2014) 513–522.
[33] R. Ghahremanzadeh, Z. Rashid, A.H. Zarnani, H. Naeimi, Synthesis of novel spirooxindoles in water by using $MnFe_2O_4$ nanoparticles as an efficient magnetically recoverable and reusable catalyst, Appl. Catal. A: Gen. 467 (2013) 270–278.
[34] Y.S. Fu, P. Xiong, H.Q. Chen, X.Q. Sun, X. Wang, High photocatalytic activity of magnetically separable manganese ferrite-graphene heteroarchitectures, Ind. Eng. Chem. Res. 51 (2012) 725–731.
[35] P. Laokul, V. Amornkitbamrung, S. Seraphin, S. Maensiri, Characterization and magnetic properties of nanocrystalline $CuFe_2O_4$, $NiFe_2O_4$, $ZnFe_2O_4$ powders prepared by the Aloe vera extract solution, Curr. Appl. Phys. 11 (2011) 101–108.
[36] M. Pagano, A. Volpe, G. Mascolo, A. Lopez, V. Locaputo, R. Ciannarella, Peroxymonosulfate-Co(II) oxidation system for the removal of the non-ionic surfactant Brij 35 from aqueous solution, Chemosphere 86 (2012) 329–334.
[37] Y.Q. Wang, R.M. Cheng, Z. Wen, L.J. Zhao, Synthesis and characterization of single-crystalline $MnFe_2O_4$ ferrite nanocrystals and their possible application in water treatment, Eur. J. Inorg. Chem. 2011(19) (2011) 2942–2947.
[38] S.M. Sun, W.Z. Wang, L. Zhang, L. Zhou, W.Z. Yin, M. Shang, Visible light-induced efficient contaminant removal by Bi_5O_7I, Environ. Sci. Technol. 43 (2009) 2005–2010.
[39] H. Kyung, J. Lee, W.Y. Choi, Simultaneous and synergistic conversion of dyes and heavy metal ions in aqueous TiO_2 suspensions under visible-light illumination, Environ. Sci. Technol. 39 (2005) 2376–2382.
[40] A.R. Negri, G. Jimenez, R.T. Hill, R.C. Francis, Caroate delignification Part 4: The generation and role of hydroxyl radicals, Tappi J. 81 (1998) 241–246.
[41] Y.H. Guan, J. Ma, X.C. Li, J.Y. Fang, L.W. Chen, Influence of pH on the formation of sulfate and hydroxyl radicals in the UV/peroxymonosulfate system, Environ. Sci. Technol. 45 (2011) 9308–9314.
[42] C.J. Liang, H.W. Su, Identification of sulfate and hydroxyl radicals in thermally activated persulfate, Ind. Eng. Chem. Res. 48 (2009) 5558–5562.
[43] G.P. Anipsitakis, D.D. Dionysiou, Radical generation by the interaction of transition metals with common oxidants, Environ. Sci. Technol. 38 (2004) 3705–3712.
[44] Y.B. Wang, H.Y. Zhao, M.F.Q. Li, J.H. Fan, G.H. Zhao, Magnetic ordered mesoporous copper ferrite as a heterogeneous Fenton catalyst for the degradation of imidacloprid, Appl. Catal. B: Environ. 147 (2014) 534–545.
[45] S. Fronaeus, J. Berglund, L.I. Elding, Iron−manganese redox processes and synergism in the mechanism for manganese-catalyzed Autoxidation of hydrogen sulfite, Inorg. Chem. 37 (1998) 4939–4944.
[46] E.G. Heckert, S. Seal, W.T. Self, Fenton-like reaction catalyzed by the rare earth inner transition metal cerium, Environ. Sci. Technol. 42 (2008) 5014–5019.
[47] L.J. Xu, J.L. Wang, Magnetic nanoscaled Fe_3O_4/CeO_2 composite as an efficient Fenton-like heterogeneous catalyst for degradation of 4-chlorophenol, Environ. Sci. Technol. 46 (2012) 10145–10153.
[48] T. Lan, L.C. Lei, B. Yang, X.W. Zhang, Z.J. Li, Kinetics of the iron(II)- and manganese(II)-catalyzed oxidation of S(IV) in seawater with acetic buffer: A study of seawater desulfurization process, Ind. Eng. Chem. Res. 52 (2013) 4740–4746.